

AN IMPROVED BEHAVIORAL MODELING TECHNIQUE FOR HIGH POWER AMPLIFIERS WITH MEMORY

N. Le Gallou*, E. Ngoya**, H. Buret*, D. Barataud**, J.M. Nebus**

* ALCATEL SPACE INDUSTRIES, 26 Av. J.F. Champollion , 31037 Toulouse Cedex, France

** IRCOM UMR CNRS 6615, University of Limoges , 123 Av. A. Thomas 87060 Limoges, France

Abstract — The introduction of frequency dependence in system level nonlinear behavioral models is of prime importance as wideband signals are going to be massively used with nonlinear SSPA . This paper describes an improved technique to model envelope memory effects for amplifiers exhibiting both high and low frequency memory.

I. INTRODUCTION

With the development of new characterization tools [1-3], new possibilities have been offered towards black box modeling of nonlinear circuits driven by modulated signals.

The major advantage of the use of black box models at system or subsystem level, is the model simplicity allowing to simulate more complicated structures like satellite payload solid state power amplifiers (SSPA) [6] with complex modulated signals (NPR, QPSK ...).

The classical well established method consisting of using AMAM AMPM curves for narrow band system level simulation is no more suitable for simulation of wideband signals because the frequency response (memory) of the amplifier has to be taken into account.

However finding an accurate technology independent relation between input and output ports of the nonlinear device is a great dilemma when nonlinear memory has to be introduced in the model. This problem has found some solutions in the case of traveling wave tube amplifiers (TWTA) [7-9] exhibiting only High Frequency memory (due to frequency limiting matching circuits). Problem becomes more difficult when both High and Low frequency Memory (due to biasing circuits) are mixed together like in solid state high power amplifiers [4][5].

Recently a new behavioral model based on Dynamic Volterra formalism has been introduced [10] for the representation of both High and Low Frequency Memory. However based on a linear mixer extraction principle of the kernels [11], this model has proved to be limited to mildly nonlinear regions (25dBc of IM3 and better) for amplifiers exhibiting strong nonlinear low frequency memory. In this article is presented an improved extraction principle of the model kernels for a better

modeling accuracy in very nonlinear multicarrier conditions.

II. PRINCIPLE OF MODEL EXTRACTION

At system level, low pass equivalent signals are used and real signals are replaced by the associated input/output complex envelopes (Fig. 1.) :

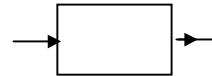
$$x(t) = \Re e[\hat{X}(t)e^{j\omega_0 t}] \quad y(t) = \Re e[\hat{Y}(t)e^{j\omega_0 t}]$$


Fig.1: Nonlinear system with memory

As formerly described in [10] the output of a nonlinear system with memory could be expressed as following :

$$\begin{aligned} \hat{Y}(t) = & \hat{Y}_{dc}(|\hat{X}(t)|) e^{j\Phi_{X(t)}} \\ & + \int_{-BW/2}^{BW/2} \hat{H}_1(|\hat{X}(t)|, f) \hat{X}(f) e^{j\Omega t} df \\ & + \int_{-BW/2}^{BW/2} \hat{H}_2(|\hat{X}(t)|, -f) e^{2\Phi_{X(t)}} \hat{X}^*(f) e^{-j\Omega t} df \end{aligned} \quad (1)$$

Where BW is the modulation bandwidth, $\hat{X}(f)$ the spectrum of input signal. $\hat{Y}_{dc}(|\hat{X}(t)|) e^{j\Phi_{X(t)}}$ is the memoryless part of the model, in fact the classical AMAM AMPM model. $\hat{H}_1(|\hat{X}(t)|, f)$ and $\hat{H}_2(|\hat{X}(t)|, -f)$ are the Dynamic Volterra Kernels accounting for nonlinear memory effects, expressing the distance from the real response to the purely static one (without memory).

Extraction of dynamic Kernels is based on a two-tone signal. The first tone, has a fixed frequency chosen at center of the amplifier bandwidth. The second tone has the same amplitude, and frequency can be swept around the first, from the left to the right for covering the amplifier band. As opposed to the extraction principle suggested

previously in [10] [11], amplitude of both frequencies must be swept from linear to strongly nonlinear region of the amplifier, as shown in Fig. 2 :

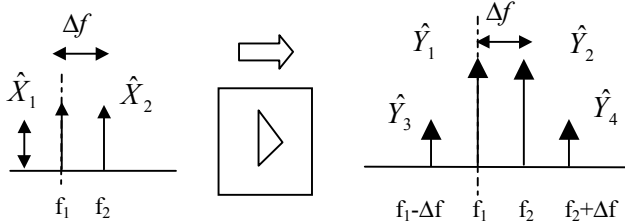


Fig. 2 : Signal setup for model extraction

The objective of the extraction is to find the two nonlinear and complex characteristics of 2 variables $\hat{H}_1(|\hat{X}(t)|, \Delta f)$ and $\hat{H}_2(|\hat{X}(t)|, -\Delta f)$. For a given frequency distance Δf , Kernels become dynamical functions of the instantaneous envelope of the input signal. However envelope of the input signal is strongly time varying. Thus, a given magnitude can be reached by different ways, depending on the amplitudes and phase between the two input tones \hat{X}_1 and \hat{X}_2 as shown in Fig. 3 :

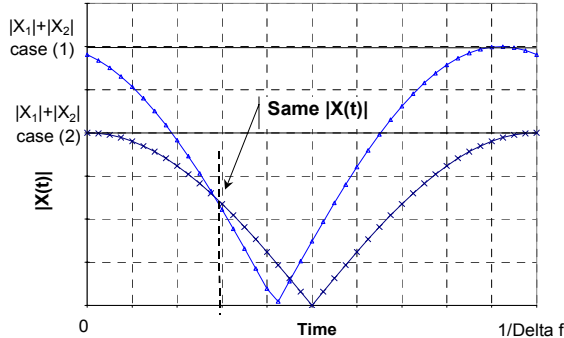


Fig. 3 : Time Domain Amplitude of Input Signal

Therefore the characteristics \hat{H}_1 and \hat{H}_2 as a function of the envelope magnitude $|\hat{X}(t)|$ can be found only in a minimum least square fitting sense, by considering all possible combinations (\hat{X}_1, \hat{X}_2) and time. One could do this by considering any functional decomposition of the characteristics. For computational efficiency reason, we propose here a piece-wise linear decomposition. The principle is as shown in Fig.4, the segments of the piece-wise characteristics are constructed recursively, starting from small signal region up to large signal.

The principle is that, for a given couple of input signal (\hat{X}_1, \hat{X}_2) , input instantaneous envelope verifies :

$$|X(t)| \leq |\hat{X}_1| + |\hat{X}_2| = X_{\max} \quad (2)$$

The first segment from 0 to X_{\max}^1 is computed by optimization of kernels values at X_{\max}^1 , with the objective that the model reproduces in a two-tone simulation the output spectrum (phases and amplitudes) of the two tones and third order intermodulation products measured on the HPA. With the first segment constructed, the second segment from X_{\max}^1 to $X_{\max}^2 = (|\hat{X}_1| + |\hat{X}_2|)_2$ is now computed the same way. This procedure is repeated forth, to cover the complete amplifier input power range, and for each frequency tone distance Δf .

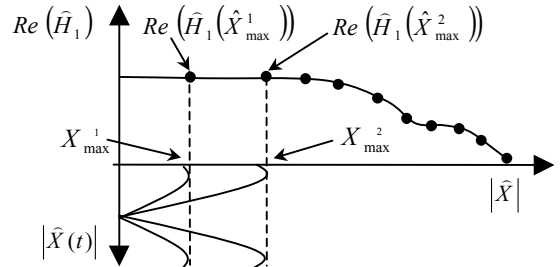


Fig. 4 : Determination of $Re(\hat{H}_1)$ point after point.

An efficient optimization procedure will yield smooth characteristics \hat{H}_1 and \hat{H}_2 versus $|\hat{X}|$ or Δf

The advantages of this method is that no a priori supposition is made on the curves \hat{H}_1 and \hat{H}_2 versus $|\hat{X}|$ or Δf . In the same way, no limitation is imposed on amplitude or phase repartition of the output spectrum : in particular low third order intermod ($2f_1-f_2$) could have a different amplitude than the high intermod ($2f_2-f_1$).

The principle of extraction, is fully applicable to data coming from circuit level simulation, when a system level representation is rewarded. Indeed amplitudes and phase of each tone at input or output of the HPA are perfectly known in a commonly used Harmonic balanced simulation.

However, situation is more difficult for an experimental extraction, because absolute measurement of scattering wave namely in terms of phase in multicarrier signals necessitates very specific measurement systems [1-3].

II. EXPERIMENTAL SETUP

For experimental extraction the proposed method is based on a modified Vector Network Analyzer (VNA), used in receiver mode, calibrated with a classical SOLT and a power calibration [11].

In this mode the analyzer can be used to measure ratios in amplitude and phase of tones at f_1 and f_2 . For third order

intermodulation (IMD), amplitude is directly measured by the VNA using the internal power reference.

However, as there is no input power at $2f_1-f_2$ and $2f_2-f_1$, ratios could not be done at this frequencies between input and output of the DUT. To resolve this problem, we have constructed a reference signal composed of all necessary tones and which is kept constant during the measurement, for a given Δf . With this technique, evolution of phase on IMDs versus input power could be stored. But the starting point of IMD phase curve versus input power (absolute phase) is not known because it is only a differential measurement. An effective de-embedding technique for absolute phase of IMDs has been found and is presented below.

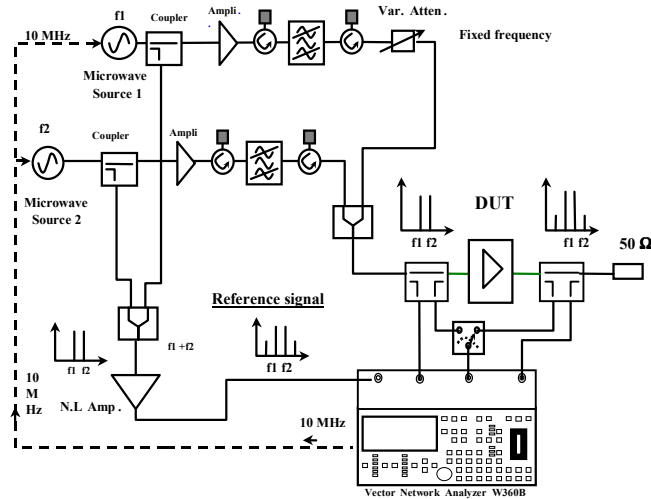


Fig. 5 : Measurement setup

III. DETERMINATION OF THIRD ORDER IMDs PHASE IN SMALL SIGNAL

The solution found to resolve this absolute phase problem is based on observations made on various nonlinear simulations of HPA, as well as measurement made with VNA.

The first observation is that input/output phase shift on second tone f_2 has an approximately constant negative slope S_{f2} when it is shifted away from f_1 (f_1 remaining constant). The reason is that an amplifier has an approximately constant group delay in its bandwidth. This result is found on circuit level simulation of the HPA as well as with VNA measurements on f_2 .

The second observation is that the phase slope of the third order IMDs are approximately related to slope on carriers as follows :

$$S_{2f_2-f_1} = 2*S_{f2} - S_{f1} \quad \text{and} \quad S_{2f_1-f_2} = 2*S_{f1} - S_{f2} \quad (3)$$

But as f_1 is kept constant :

$$S_{2f_2-f_1} = 2*S_{f2} \quad \text{and} \quad S_{2f_1-f_2} = -S_{f2} \quad (4)$$

The last observation is that phase of IMDs for tones very close to each other, can be considered equal and calculated using the memoryless AM/AM AM/PM Model.

Thus by exploiting these three above observations, it is possible to de-embed the absolute phase of the third order IMD tones. Fig.6 shows the comparison of phases found using harmonic balance simulation on the design circuit of an HPA and the above described technique. The difference observed is very small (less than 10%) over +/- 250 MHz.

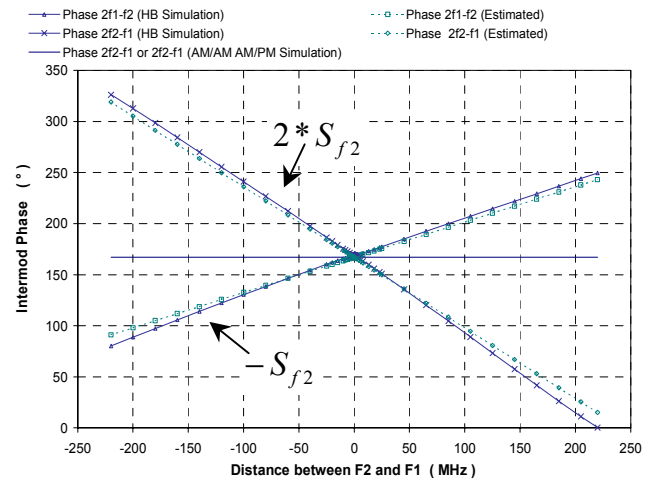


Fig. 6 : IMDs Phase for a Small Input Power (absolute phase)

For the experimental exploitation, AM/AM AM/PM curves and the slope S_{f2} are directly measured on HPA, with VNA. Absolute phase on third order intermods is then calculated in small signal conditions. By adding the differential value versus input power measured using setup Fig. 5, it is possible to have a good approximation of absolute phase on IMDs for each input power.

IV. APPLICATION TO A C-BAND 10W HPA

Extraction of the model has been applied to a C-Band HFET based nonlinear amplifier of 10W output power. This amplifier exhibits nonlinear memory effects.

The method has been first applied to the circuit design using HB simulation. Center frequency is 3.8 GHz. Results are given in Fig. 7 where a very good agreement between HB simulations and behavioral model is shown. In particular low frequency variations of IM3 are very well modeled.

The method has been then applied to the real circuit using experimental data from setup Fig.5. An approximation of absolute phase of IMDs has been determined using method described section III. Fig. 8 gives a comparison of IM3 measured on the circuit module and IM3 given by the model in a system level

two-tone simulation. A good agreement is found, in particular nonlinear resonance are well reproduced.

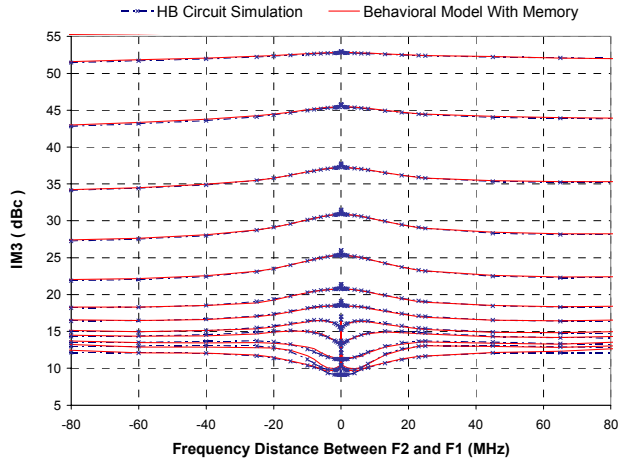


Fig. 7 : IM3 of HPA Model / HB simulation

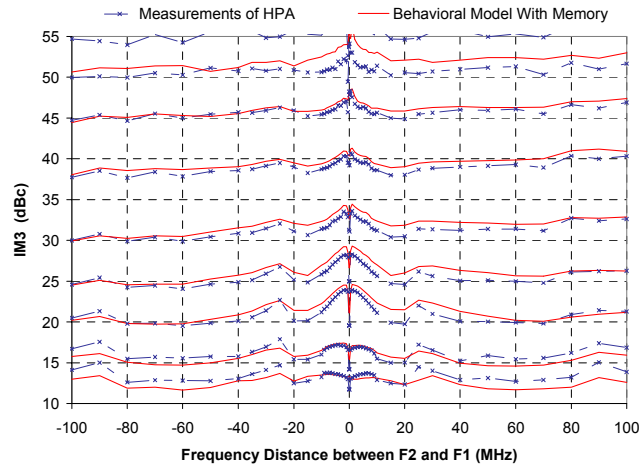


Fig. 8 : IM3 of HPA Model / Measurements

Finally to validate the approach the Noise Power Ratio (NPR) over a 20MHz bandwidth of the circuit has been simulated using the behavioral model, and has been compared to measurements as well as to the classical AMAM AMPM Model (Fig.9). The new model exhibits an improved accuracy for NPR simulation.

V. CONCLUSION

An improved behavioral modeling technique based on a Dynamic Volterra Formalism has been presented. With this method frequency nonlinear behavior of a C-band HPA has been reproduced with a good accuracy using data coming from circuit level simulation as well as data coming from direct measurements of HPA module.

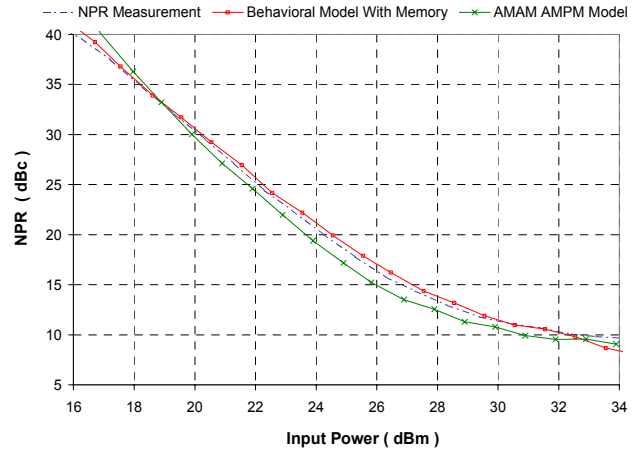


Fig. 9 : NPR of HPA Model / Measurement

REFERENCES

- [1] J. Verspecht, P. Debie, A. Barel and L. Martens, "Accurate on-wafer measurement of phase and amplitude of the spectral components of incident and scattered voltage waves at the signal ports of a non-linear microwave device", IEEE MTT-S IMS Digest Orlando May 1995, pp. 1029-1032.
- [2] D. Barataud, & Al, "Measurements of time domain voltage/current waveforms at R.F. and microwave frequencies, based on the use of a Vector Network Analyzer, for the characterization of nonlinear devices. Application to high efficiency power amplifiers and frequency multipliers optimization". IEEE Trans. Instrum. and Measurement, vol. 47, n°5, Oct. 1998, pp.1259-1264.
- [3] C.J. Clark, G. Chrisikos, & Al., "Time-Domain Envelope Measurement Technique with Application to Wideband Power Amplifier Modeling", IEEE Trans. Microw. Theory Techn., vol. 46, no. 12 December 1998, pp2531-2540.
- [4] W. Bösch, G. Gatti, "Measurement and simulation of Memory effects in predistortion linearizers", IEEE Trans. Microw. Theor. Techn., vol. 37 no 12, dec 1989.
- [5] N. Le Gallou, & Al, "Large Signal Characterization and Modeling of Power Amplifiers Driven by Modulated Signals, Part II", EuMW Workshop 1 "New Large Signal Characterization and Modeling Technique for RF and Microwave Circuits and Systems", Paris 2-6 Oct. 2000.
- [6] M. Zoyo, N. Cartier & Al, "X-Band 22W SSPA for Earth observation satellites", GAAS 1999 Digest pp 190-193.
- [7] C.P. Silva, C.J. Clark, & Al, "Optimal Filter Approach for Nonlinear Power Amplifier Modeling and Equalization", 2000 IEEE MTT-S Digest, pp 437-440.
- [8] A. Saleh, "Frequency-independent and frequency-dependent models for TWT amplifiers", IEEE Trans. Communications, COM-29, pp.1715-1720, Nov. 1981
- [9] M. T. Abuelma'atti, "Frequency-dependent Nonlinear Quadrature Model for TWT amplifiers", IEEE Trans. Communications, COM-32, pp.982-986, Aug. 1984.
- [10] E. Ngoya, N. Le Gallou, & Al, "Accurate RF and Microwave System Level Modeling of Wide Band Nonlinear Circuits", 2000 IEEE MTT-S Digest.
- [11] N. Le Gallou, D. Barataud, & Al., "A novel measurement method for the extraction of dynamic volterra kernels of microwave power amplifiers", EuMW GaAs 2000, Paris 2-6 Oct. 2000.